# Prospects for near-infrared characterisation of hot Jupiters with the VLTI Spectro-Imager (VSI)

S. Renard[a], O. Absil[a], J.-P. Berger[a], X. Bonfils[b], T. Forveille[a], F. Malbet[a]

[a]Laboratoire d'Astrophysique de l'Observatoire de Grenoble (LAOG), France;
[b]Observatorio Astronomico de Lisboa, Lisboa, Portugal

## ABSTRACT

In this paper, we study the feasibility of obtaining near-infrared spectra of bright extrasolar planets with the 2nd generation VLTI Spectro-Imager instrument (VSI), which has the required angular resolution to resolve nearby hot Jupiters from their host stars. Taking into account fundamental noises, we simulate closure phase measurements of several extrasolar systems using four 8-m telescopes at the VLT and a low spectral resolution ($R = 100$). Synthetic planetary spectra from Barman et al are used as an input. Standard chi2-fitting methods are then used to reconstruct planetary spectra from the simulated data. These simulations show that low-resolution spectra in the H and K bands can be retrieved with a good fidelity for half a dozen targets in a reasonable observing time (about 10 hours, spread over a few nights). Such observations would strongly constrain the planetary temperature and albedo, the energy redistribution mechanisms, as well as the chemical composition of their atmospheres. Systematic errors, not included in our simulations, could be a serious limitation to these performance estimations. The use of integrated optics is however expected to provide the required instrumental stability (around $10^{-4}$) to enable the first thorough characterisation of extrasolar planetary emission spectra in the near-infrared.

**Keywords:** hot Jupiters - Interferometry - VSI

## 1. INTRODUCTION

Since the discovery by Mayor & Queloz ([1]) of the first exoplanet around 51 Pegasi, the study of planetary systems receives an increasing attention, with the development and test of more and more detection techniques. Among the direct detection techniques, interferometry is one of the most promising for the near future. It already provides the required angular resolution, but the dynamic range needs to be improved. The detection and characterization of extrasolar planets is one of the main science cases of the 2nd generation VLTI Spectro-Imager instrument (VSI).

At a distance of $a \approx 0.05$ AU, the most of the detected exoplanets, called hot Jupiters, receive from their parent star about $10^4$ times the amount of radiation intercepted by Jupiter from our Sun. So close from the star, they are also believed to be tidally locked such that half of the planet faces permanently the star while the other half stays in the dark. The fraction of incident light absorbed by the atmosphere – parametrised by its albedo $A$ – heats the planets. This heat is redistributed to the night side by strong wind and reradiated by the planet. Besides providing their heat source, the strong radiation illuminating hot Jupiters also structures their atmosphere. It suppresses the convection to depths well below the photosphere, leading to a fully radiative photosphere across most of the day side ([2]). Whether silicate clouds can persist in the photosphere then results from the competition between the sedimentation and advective timescales. The sedimentation timescale of radiative photosphere is short and the winds are believed not to be strong enough to prevent dust from settling.

Further author information: (Send correspondence to S.R.)
S.R.: E-mail: Stephanie.Renard@obs.ujf-grenoble.fr, Telephone: +33 (0)4 76 63 58 40
O.A. : E-mail: Olivier.Absil@obs.ujf-grenoble.fr
J.P.B.: E-mail: Jean-Philippe.Berger@obs.ujf-grenoble.fr
X.B.: E-mail : xavier.bonfils@oal.ul.pt
T.F.: E-mail: Thierry. Forveille@obs.ujf-grenoble.fr
F.M.: E-mail : Fabien.Malbet@obs.ujf-grenoble.fr

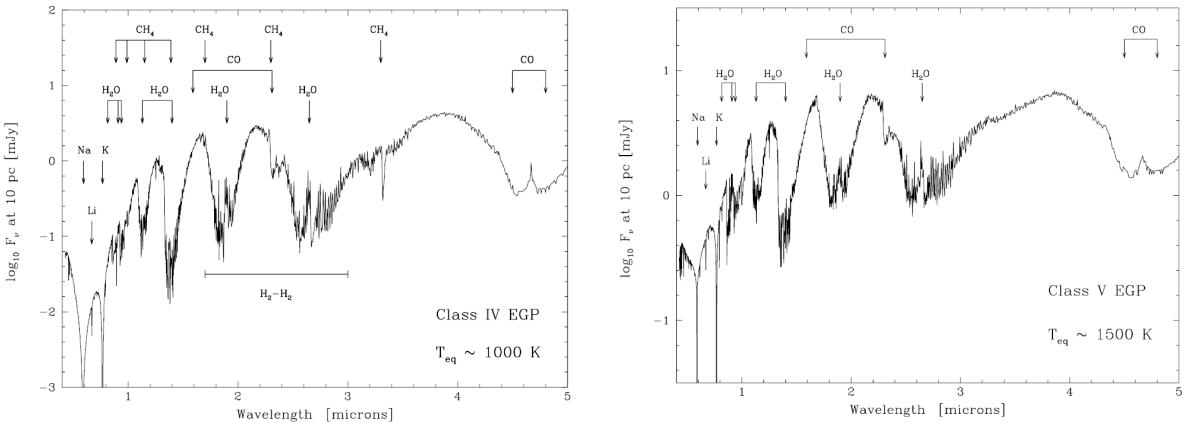


Figure 1. Model fo spectra for hot Jupiters, with $T_{eq} = 1000$K and 1500K, orbiting a Sun-like star. Important changes in abundances and band strength are seen between both cases ([3])

Hence, the atmospheres of hot Jupiters are pictured as being free of clouds. Finally to reproduce hot-Jupiter spectra, one has to take their chemical composition into account. As the opacity of each species regulates the emergent flux as a function of wavelength, their emergent spectra strongly depart from an ideal black body assumption. They display large molecular bands and spectral features (see Figure 1).

The transit technique revolutionised the fild of exoplanetology, was a breakthroughh to peer into hot Jupiters' structure and already gave a glimpse about their composition. However, the error bars remains large to discriminate between different models and most of the planetary spectrum remains unknown. Particulary, the $1-2.4$ $\mu$m spectrum is very rich in spectral information and may provide unprecedented constraints on our understanding of planetary atmosphere. VSI will have the ability to observe hot Jupiters in J, H and K bands, with a low ($R = 100$) or medium ($R = 1000$) resolution. Model fitting of low-resolution spectra will give a measurement of their albedo and test the cloud-free assumption. The phase dependance of the measured signal shall constrain the heat redistribution (throught the temperature across the surface) and the weather conditions. At medium resolution, it will be possible to measure the abundance of CO and test the presence of $CH_4$. Contrarily to current characterisation techniques, VSI will not be restricted to transiting planets. The sample of favourable targets counts already 7 planets today and may count at least twice this number at the time of VSI will be on the sky. Therefore, VSI will not only enhance our knowledge on few transiting planets, it will also move the picture to the statistical stage and literally enable the comparative exoplanetology.

The goal of this work is to study the feasibility of obtaining near-infrared emission spectra of bright extrasolar giant planets (EGPs) with VSI. In Section 2, we explain the method used for the simulation, from the choose of the targets to the step of the simulations. Section 3 contains the results of the simulation, whereas Section 4 are the discussion and the conclusions.

## 2. METHOD

In ordre to assess the feasability of planetary spectra characterisation with VSI, we use in the following simulations the synthtic spectra developped by Burrows ([4]). The latest models for the brightest and closest hot Jupiters have been kindly provided by T. Barman and are illustrated Figure 2.

### 2.1 Choice of targets

To determine the feasibility of EGP spectroscopy with VSI, we simulate interferometric observations of several EGPs that have been discovered by radial velocity surveys.

The suitable targets for an interferometric study are the hot extrasolar giant planets that orbit close to their parent stars, for which the star/planet contrast does not exceed a few $10^4$ in the near-infrared. Another criterion is that the target must be close enough so that VSI, with its angular resolution of a few milli-arcsec, can resolve

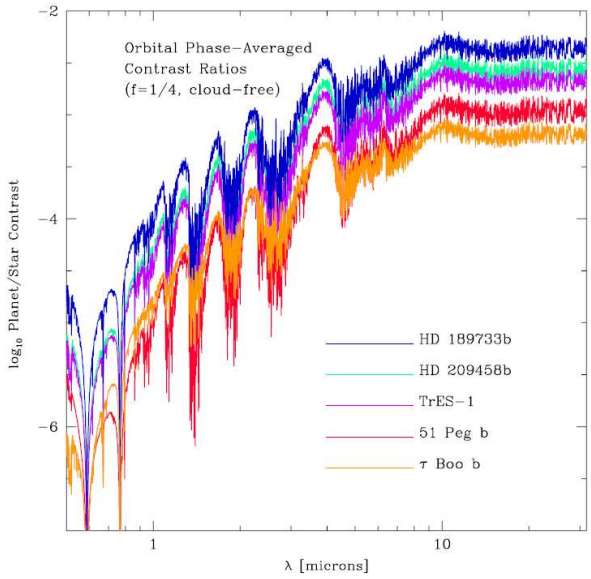


Figure 2. Planet-to-star contrast ratio for few favourable exoplanet ([5])

Table 1. Parameters of the host stars for the selected extrasolar planetary systems ([7,8]). The stellar radius is given in units of the solar radius. "Size" is the expected stellar angular diameter in milliarcsec.

| Star name | RA (J2000) | Dec (J2000) | $m_V$ | $m_J$ | $m_H$ | $m_K$ | Dist (pc) | Spec. type | Star radius | Size (mas) |
|---|---|---|---|---|---|---|---|---|---|---|
| $\tau$ Boo | 13h47m17s | +17 ° 27'22" | 4.5 | 3.6 | 3.5 | 3.5 | 16 | F7V | 1.43 | 0.43 |
| HD 179949 | 19h15m33s | -24 ° 10'45" | 6.3 | 5.3 | 5.1 | 4.9 | 27 | F8V | 1.23 | 0.21 |
| HD189733 | 20h00m44s | +22 ° 42'39" | 7.7 | 6.1 | 5.6 | 5.5 | 19 | K1-2V | 0.777 | 0.19 |
| HD 73256 | 08h36m23s | -30 ° 02'15" | 8.1 | 6.7 | 6.4 | 6.3 | 37 | G8/K0 | 0.99 | 0.13 |
| 51 Peg | 22h57m27s | +20 ° 46'07" | 5.5 | 4.7 | 4.2 | 3.9 | 15 | G2IV | 1.15 | 0.36 |
| HD 209458 | 22h03m10s | +18 ° 53'04" | 7.7 | 6.6 | 6.4 | 6.3 | 47 | G0V | 1.15 | 0.11 |

the star-planet system. Typically, hot Jupiter systems further than 50 pc fall outside the resolving power of VSI. Finally, we have restricted the list target to declinations ranging between -84 ° and +36 ° , in order to be observable from Cerro Paranal.

A list of six targets, based on these criteria, has been compiled in Table 1. The properties of the planetary companions are listed in Table 2. These targets were expected to give the better results in terms of detectability. In order to carry out performance simulations we ave estimated the temperature of these extrasolar planets based on the radiative equilibrum of a grey body ($T_p = T_*(1-A_b)^{1/4}\left(\frac{R_*}{2a}\right)^{1/2}$) and their radii assuming a mean density of 0.7 g cm$^{-3}$ ([6]).

## 2.2 The method : differential closure phases

Because hot Jupiters are very close to their parent star, they are the planets with both the most important source of heat and the planets that most reflect the starlight, in brief, they are the most luminous amoung known exoplanets. Nevertheless, as one can guess from the scarse observations, they remain very difficult targets for direct observations. The typical contrast between hot Jupiters and their parent star ranges from $10^{-6}$ in the visible to $10^{-3}$ beyond 10 $\mu$m. In the wavelength domain of VSI, common hot Jupiters have a typical contrast of $10^{-4}$ and the best targets reach a contrast of $10^{-3}$ (see Figure 2).

Table 2. Parameters of the selected extrasolar planets ([7,8]). The planetary radii are derived from transit measurements when available, while the values followed by an asterik are estimates using a mean planet densitiy of 0.7 g cm$^{-3}$ ([6]) and a upper limit of 1.5R$_J$. The semi-major axis is given in AU and in mas, assuming the planet to be at maximum elongation. The estimate temperature and flux of the hot Jupiters are computed using a grey body assumption with a Bond albedo of 0.1. The stellar and planetary fluxes, as well as the planet/star contrast, are given in the centre of the K band.

| Planet name | M sin $i$ (M$_J$) | Radius (R$_J$) | Temp (K) | axis (AU) | axis (mas) | period (days) | F$_*$ (Jy) | F$_p$ (Jy) | Contrast (K band) |
|---|---|---|---|---|---|---|---|---|---|
| $\tau$ Boo b | 3.9 | 1.5* | 1607 | 0.046 | 2.95 | 3.31 | 27.3 | 8.1e-3 | 3.0e-4 |
| HD 179949 b | 0.92 | 1.2* | 1533 | 0.045 | 1.67 | 3.09 | 6.61 | 2.2e-3 | 3.4e-4 |
| HD189733 b | 1.15 | 1.16 | 1180 | 0.031 | 1.61 | 2.22 | 3.60 | 9.4e-3 | 2.6e-4 |
| HD 73256 b | 1.87 | 1.5* | 1296 | 0.037 | 1.01 | 2.55 | 1.82 | 4.3e-3 | 2.3e-4 |
| 51 Peg b | 0.47 | 0.9* | 1265 | 0.052 | 3.54 | 4.23 | 17.3 | 2.3e-3 | 1.3e-4 |
| HD 209458 b | 1.32 | 1.32 | 1392 | 0.045 | 0.96 | 3.52 | 1.81 | 4.8e-3 | 2.6e-4 |

Observations at such contrast are challenging and different startegies are currently investigated. Finally, it has been proposed that the resolving power of interferometry provides the means to achieve observations of hot Jupiters and two approaches have been investigated: differential phase and differential closure phase. The first approach measures the photo-centre of the planet+star system (as a function of wavelength) whereas the second measures the fraction of light that is not point-symmetric (as a function of wavelength too). In both cases, it provides the differential planet to star contrast ratio as a function of wavelength.

When a star comes with a faint companion and when both fall in the filed of view of an interferometer, their fringe pattern sum together incoherently. Hence the presence of a planet decreases the fringe contrast and modulates the phase by tiny amounts (see Figure 3). From the ground, the main problem is the Earth atmoshpere, which absorption varies chromatically and on time scales shorter than the time required to perform the observations. Sadly, such wavelength dependent phase shifts prevent the use of "differential phase" technique for high contrast observations. Only the use of interferometry with closure phase presents the nice property of cancelling atmospheric systematics. In fact, with three or more telescopes, one can build an alternative interferometric observable that is robust to phase shifts: the closure phase. As shown Figure 4, a differential optical path above one telescope (here the $2^{nd}$) introduced phase shifts on fringes measured on two baselines (here baselines $b_{1-2}$ and $b_{2-3}$). Also, the phase shifts have opposite signs and cancells when sums together. Since the reasoning holds for a phase delay introduced above any of the telescope, the sum of phases measured on baselines $b_{1-2}$, $b_{2-3}$ and $b_{1-3}$ cancels phase systematics. Actually, the closure phase technique does not only cancel the phase shifts introduced by the atmosphere but also the ones introduced by the instrumental optics, up to the recombination. After the recombination, the use of Integrated Optics is then a key technology to minimise the instrumental phase shifts.

Therefore, differential closure phase appears to be one of the best methods to obtain medium-resolution near-infrared spectra of known hot EGPs, because it is very sensitive to faint companions while not corrupted by random atmospheric phase fluctuations.

### 2.3 Steps of the simulation

To perform the detection of exoplanets from closure phase data, we will rely on model fitting. The resort to image reconstruction is not needed in our case, as the system of a hot Jupiter plus a star is just the case of a binary, though a highly contrasted one. The performance simulations will therefore consist in the following steps:

1. Simulate the observation of star-planet system under typical conditions : we assume that the system is observed three consecutive nights with the four UTs and that four data points are required each night at a rate of one data point per hour. Each data point consist in a 10-min n-source integration, and is following by calibration measurements (not simulated here).

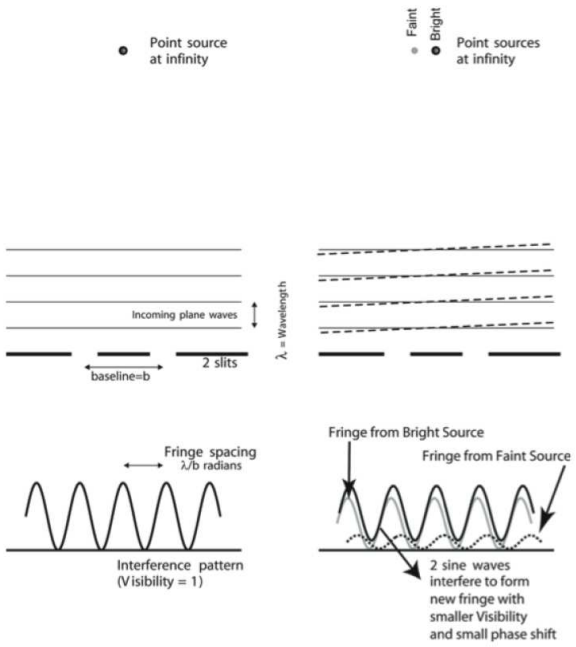


Figure 3. The figure illustrates how the presence of a planet modulates the phase of interferometric fringes ([9])

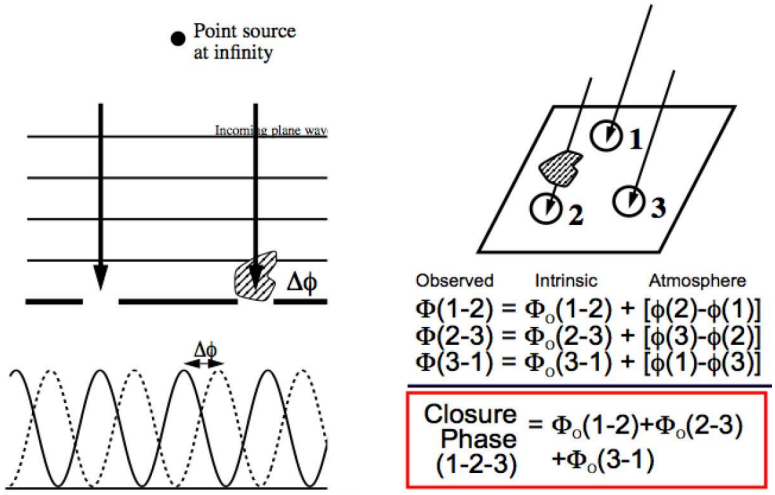


Figure 4. The figure illustrates how a phase delay introduced above a telescope can be canceled in the closure phase quantity. The closure phase equals the sum of phases measured along baselines formed by at least three telescopes ([10]).

2. Estimate the fundamental noises (shot noise and detector noise) for each individual measurement, using the lowest spectral resolution of VSI ($R = 100$). The error bars on individual data points typically range between $3 \times 10^{-5}$ and $10^{-4}$ radians for stellar magnitude between 3.5 and 6.5 in the K band. Using these estimated error bars, we draw random data points using a gaussian distribution centred around the noiseless closure phase and with a standard deviation equal to the error bar. This result in a collection of data points with associated error bars (see Figure 6), which are used as an input for the fitting procedure.

3. Fit the simulated observations and their associated error bars with a model for the closure phase of the planetary system as a function of time. The time evolution of the closure phase simultaneously capture the movement of the star-planet system on the night sky and revolution of the planet around its host star (typical period of 3 days for the systems considered here).

## 3. RESULTS

### 3.1 Fitting the orbital parameters

Various free parameters can be used to perform the fit to the simulated closure phase observations. Here, we select the three most important parameters that are not known from radial velocity measurements : the planet/star contrast, the orbital inclination and the position angle of the orbit on the plane of the sky (counted East of North)*. In first step, we fit the three parameters globally on the whole spectral domain. Because the contrast significantly changes between individual spectral channels, we replace the first fitting parameter (the contrast) by the planetary radius. Fitting the planet/star contrast is indeed equivalent to fitting a planetary radius in each channel if one makes the following assumptions :

- The thermal emission follows a grey body emission law.
- The albedo is constant and fixed to given value (0.1 in our case).
- The temperature of the planet is computed from radiative equilibrum.

It must be noted that the choice to compute the fit on the planet radius rather than on the albedo is due to the fact that, when fitting the data, the albedo changes rapidly for small variations of the radius and can quickly reach non-physical values if a poor estimation of the radius is chosen –a problem which is not present when fitting the planetary radius. This come from the fact that $F_{thermal} \propto (1 - A_b)^{1/4} R_p^2$, so a variation of $R_p$ induces a bigger influence on $F_{thermal}$ than a variation of $A_b$.

The fit is performed in two successive steps. In a first step, we investigate the hole parameter space and compute the $\chi^2$ between the observations and the model for a whole range of values for the radius, inclination and position angle. From the resulting $\chi^2$ hypersurface, we determine an approximate position for the global minimum, which we will use as an initial guess in the second step of the fit. The graphical representations of the $\chi^2$ cube (see Figure 5) allow us to evaluate the sharpness of the $1/\chi^2$ peak and the possible occurence of local minima. The second step consists in a classical Levenberg-Marquardt minimisation of the $\chi^2$ with the three free parameters. This step usually converges quickly towards the best-fit solution, as the initial guess is generally robustly determined during the first step of the fitting procedure.

While the output best-fit radius does not have a real physical meaning under the present asumptions (grey body with fixed albedo and temperature), the inclination and position angle of the orbit are generally well reproduced by the fitting procedure, both in the H and in the K band (see Table 3 & 4). It must be noted that this two parameters are generally unknown for the simulated planets, so that arbitrary values have been used in this study.

*The latter is actually equivalent to the longitude of the ascending node of the orbit with respect to the plane of the sky.

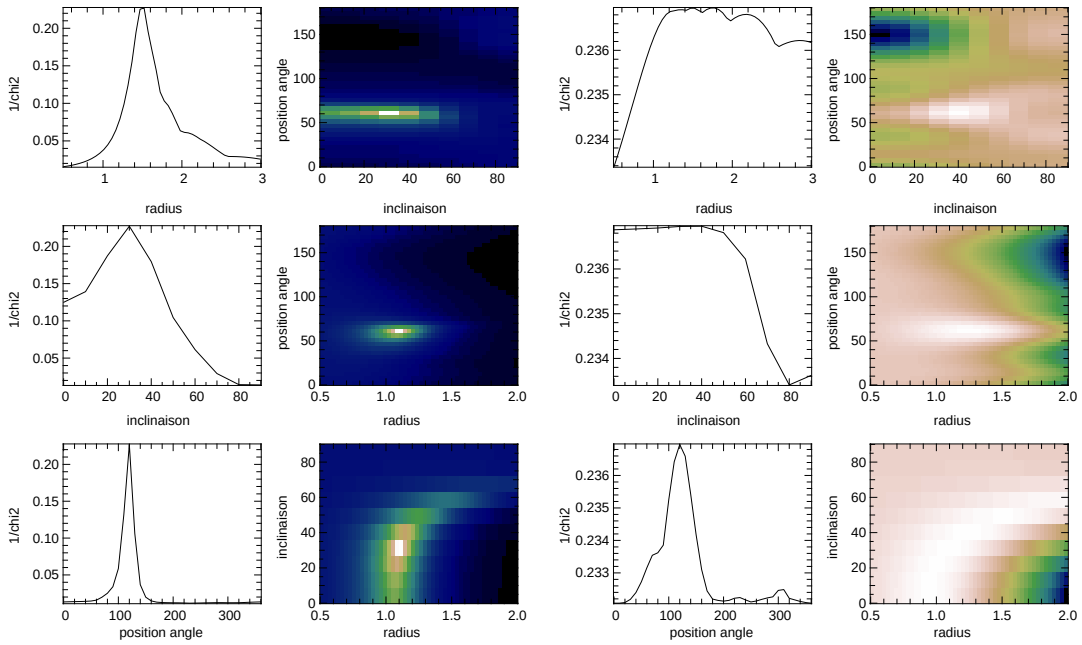


Figure 5. Graphical representations of the $\chi^2$ cube between the simulated observations and the model for a whole range of values for the three free parameters : the radius, the inclination and the position angle (left : $\tau$ Boo, right : HD 73256).

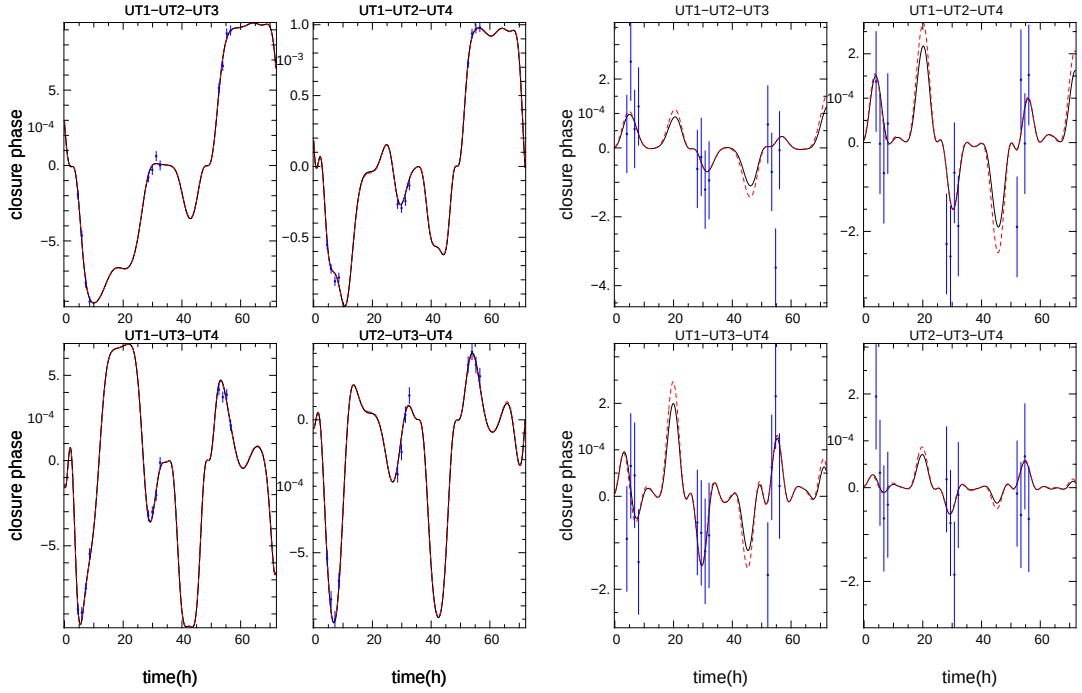


Figure 6. Simulated observations of two extrasolar planetary systems (left : $\tau$ Boo, right : HD 73256) using VSI with 4 UTs. The data points with their associated bars (in blue) are shown separately for the four triplets of baselines. The underlying black curve represents the noiseless closure phase signal of the extrasolar planet for each triplet, while the red curve represents the best fit to the simulated data, as described in section 3.1. The simulations are performed in the band K.

Table 3. Results of the orbital fit for the 6 selected exoplanets in K band

| | $\tau$ Boo b | HD 179949 b | HD 189733 b | HD 73256 b | 51 Peg b | HD 209458 b |
|---|---|---|---|---|---|---|
| inclination | 30 | 45 | 85.76 | 30 | 75 | 86.929 |
| best fit | 28.74 | 50.02 | 70.13 | -4.83 | 75.28 | 87.86 |
| error bar | 0.63 | 5.67 | 11.08 | 326.29 | 2.29 | 6.91 |
| position angle | 120 | 60 | 90 | 120 | 150 | 0 |
| best fit | 119.87 | 59.91 | 96.78 | 110 | 150.13 | 336.09 |
| error bar | 0.36 | 2.19 | 6.53 | 10.37 | 2.10 | 7.73 |

Table 4. Results of the orbital fit for the 6 selected exoplanets in H band

| | $\tau$ Boo b | HD 179949 b | HD 189733 b | HD 73256 b | 51 Peg b | HD 209458 b |
|---|---|---|---|---|---|---|
| inclination | 30 | 45 | 85.76 | 30 | 75 | 86.929 |
| best fit | 30.47 | 28.60 | 98.67 | 43.22 | 45.93 | 80.05 |
| error bar | 0.56 | 11.31 | 25.61 | 21.61 | 8.72 | 14.17 |
| position angle | 120 | 60 | 90 | 120 | 150 | 0 |
| best fit | 119.62 | 59.33 | 87.21 | 122 | 156.27 | 331.07 |
| error bar | 0.43 | 2.15 | 11.28 | 7.38 | 6.50 | 9.96 |

### 3.2 Fitting the planetary spectra

In a second step, we fix the best-fit orbital parameters obtained under the black body assumption and perform a fit on the only planetary radius individually for each spectral channel. In this step, we allow the planetary radius to change across the various spectral channels, using a black body assumption on each individual channel. The obtained planetary radii are then converted to the value of the planet/star contrast, which is the interesting quantity in this case. This fit is illustrated in Figure 7 for the K band and in Figure 8 for the H band.

## 4. DISCUSSION AND CONCLUSION

From the result of the fit of the planetary spectra, it becomes evident that VSI will be a powerful tool to characterize hot Jupiters. The simultaneous measurement of the contrast at various wavelengths will provide an insight into the thermal, physical and dynamical structure of their atmospheres. In particular, the slope of the spectrum in H and K band will directly inform on the presence of $CH_4$ in the planetary atmosphere, while the CO absorption feature around 2.3 $\mu$m could also be detected around some of the selected targets. Furthermore, the reapeated observations at various orbital phases will provide an important information to constrain the heat distribution mechanisms by measuring the temperature and atmospheric composition around the planet.

We note that the simulated observations are more successful and constraining if the star-planet system is close to the observer ($\leq 20pc$). For such targets, the VLTI angular resolution well matches the star-planet separation and the planet is bright enough to provide a good SNR. It is thus recommended to choose the closer systems as the first targets of VSI.

In the light of these results, one can safely conclude that the prime criterion for the selection of additional targets is the magnitude of the host star: it drives the signal to noise ratio on the closure phases and therefore the quality of the fit of the planetary data. The semi-major axis of the planetary orbit, or more precisely, the temperature of the planetary companion, is of course another critical parameter, as well as its radius (which is generally poorly known). From these observations, additional targets can be proposed for the VSI exoplanet sampel such as HD 75286 b and HD 160691 d (from the hot Jupiter family) or 55 Cnc e (a hot Neptune). All these give satisfactory results when reapeatingg the above simulation procedure, yet with larger relative error bars on the measured planet/star contrast. A few other planets may be added to the list in the coming month/year.

Systematic errors, not included in our simulations, could be a serious limitation to these performance estimations. The use of integrated optics is however expected to provide the required instrumental stability (around $10^{-4}$) to enable the first thorough characterisation of extrasolar planetary spectra in the near-infrared.

The direct detection of hot Jupiters is undoubtely one of the most challenging VSI programs. This program was already one of AMBER's goal. However VSI intrinsic design offers multiple improvements with respect to AMBER which rely on two main axis :

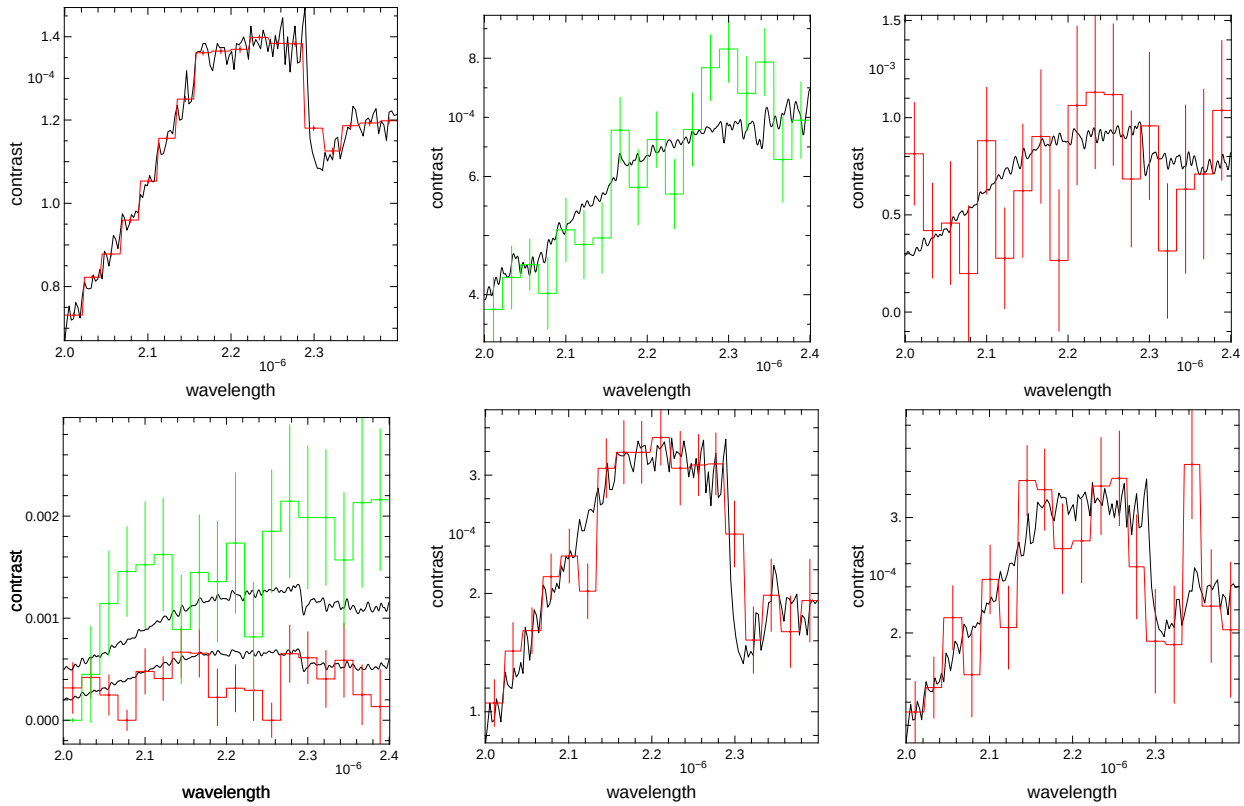


Figure 7. Fit to the planet/star contrast from the simulated closure phase data in K band (from left to right and top to bottom : $\tau$ Boo, HD 179949 b, HD 189733 b, HD 73256 b, 51 Peg b and HD 209458 b). Red curves are used for the best-fit model when the input synthetic spectrum assumes heat redistribution around the whole planet, while green curves are used when the input spectrum assumes heat redistribution on the day side only.

- improvement in the observables signal to noise and accuracy : with a heart made of an integrated optics circuit in which the incoming beams are spatially filtered and routed so that each of the 4UT beams are carefully interfered with each other, the intrinsic stability of VSI is much higher than a classical bulk optics solution like AMBER. Moreover, unlike AMBER, VSI has included in its study an internal fringe tracker located as close as possible to the science instrument in order to control the stabilisation of the fringes and allow cophasing.

- increasing the number of simultaneous points: using 4 telescopes allows 4 closure phases to be measured simultaneously while AMBER only permits one such measurement. This simultaneity reduces time dependant drifts, improved the calibration and permits to constrain the flux ratio by 4 points in a single measurements instead of 1 for AMBER, improving dramatically the quality of the fit.

## REFERENCES


[1] Mayor, M. and Queloz, D., "A Jupiter-Mass Companion to a Solar-Type Star," *Nature* **378**, 355–+ (Nov. 1995).

[2] Guillot, T., Burrows, A., Hubbard, W. B., Lunine, J. I., and Saumon, D., "Giant Planets at Small Orbital Distances," *Astrophysical Journal* **459**, L35+ (Mar. 1996).

[3] Sudarsky, D., Burrows, A., and Hubeny, I., "Theoretical Spectra and Atmospheres of Extrasolar Giant Planets," *Astrophysical Journal* **588**, 1121–1148 (May 2003).

[4] Barman, T. S., Hauschildt, P. H., and Allard, F., "Irradiated Planets," *Astrophysical Journal* **556**, 885–895 (Aug. 2001).

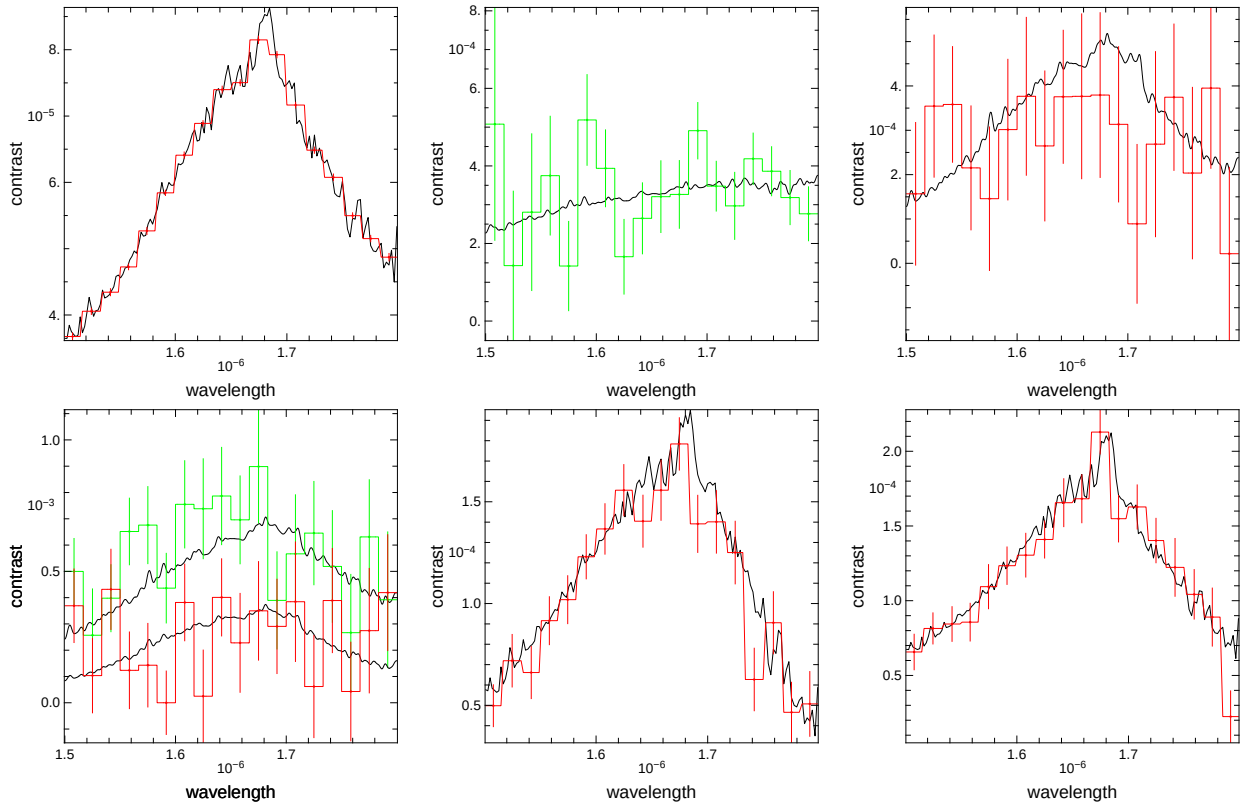


Figure 8. Fit to the planet/star contrast from the simulated closure phase in the H band (same conventions as in Figure7).


[5] Burrows, A., Hubeny, I., and Sudarsky, D., "A Theoretical Interpretation of the Measurements of the Secondary Eclipses of TrES-1 and HD 209458b," *Astrophysical Journal* **625**, L135–L138 (June 2005).

[6] Bouchy, F., Udry, S., Mayor, M., Moutou, C., Pont, F., Iribarne, N., da Silva, R., Ilovaisky, S., Queloz, D., Santos, N. C., Ségransan, D., and Zucker, S., "ELODIE metallicity-biased search for transiting Hot Jupiters. II. A very hot Jupiter transiting the bright K star HD 189733," *Astron. & Astrophys.* **444**, L15–L19 (Dec. 2005).

[7] Butler, R. P., Wright, J. T., Marcy, G. W., Fischer, D. A., Vogt, S. S., Tinney, C. G., Jones, H. R. A., Carter, B. D., Johnson, J. A., McCarthy, C., and Penny, A. J., "Catalog of Nearby Exoplanets," *Astrophysical Journal* **646**, 505–522 (July 2006).

[8] Schneider, J., "The Extrasolar Planet Encyclopedia," (2007). http://www.exoplanet.eu.

[9] Beuzit, J.-L., Mouillet, D., Oppenheimer, B. R., and Monnier, J. D., "Direct Detection of Exoplanets," in [*Protostars and Planets V*], Reipurth, B., Jewitt, D., and Keil, K., eds., 717–732 (2007).

[10] Lawson, P. R., ed., [*Principles of Long Baseline Stellar Interferometry*], JPL Publication, Pasadena (2000).